

# Order- $v^2$ relativistic corrections to heavy-quark fragmentation into $P$ -wave quarkonium states

Sai Cui<sup>(a)</sup>, Sheng-Juan Jiang<sup>(a)</sup>, Guang-Zhi Xu<sup>(a),\*</sup> and Kui-Yong Liu<sup>(b,a),†</sup>

<sup>(a)</sup>School of Physics, Liaoning University, Shenyang 110036, China

<sup>(b)</sup>School of Physics and Electronic Technology, Liaoning Normal University, Dalian 116029, China

\*Corresponding author. Email: xuguangzhi@lnu.edu.cn

†Corresponding author. Email: liukuiyong@lnu.edu.cn

February 6, 2026

## Abstract

Within the framework of nonrelativistic QCD (NRQCD) factorization, and based on the Collins–Soper operator definition of fragmentation functions, we present a systematic calculation of the fragmentation functions for a heavy quark fragmenting into color-singlet  $P$ -wave quarkonium states. After reproducing and confirming the known leading-order results, we further compute the relativistic corrections up to order  $\mathcal{O}(v^2)$ . Our analysis applies both to quarkonium systems composed of heavy quarks with the same flavor and to  $B_c$ -type mesons formed by heavy quarks of different flavors. Numerical results show that, for all color-singlet  $P$ -wave channels, the  $\mathcal{O}(v^2)$  relativistic corrections give sizable negative contributions over most of the momentum-fraction  $z$  region. We further compute inclusive cross sections for  $P$ -wave quarkonium plus charmed hadrons in  $e^+e^-$  annihilation via the single photon process up to  $\mathcal{O}(v^2)$  by applying our obtained fragmentation functions, and the resulting predictions are consistent with the full fixed-order results in the high-energy region.

**Keywords:** quarkonium; fragmentation function; NRQCD factorization; relativistic corrections

## I. Introduction

In high-energy collisions, the production of hadrons with large transverse momentum is dominated by parton fragmentation. In the context of heavy quarkonium production, the underlying production mechanisms and factorization properties have been extensively investigated, together with higher-order QCD and relativistic corrections in various channels [1–9]. According to the QCD factorization theorem, the corresponding differential cross sections can be expressed as convolutions of partonic production rates and fragmentation functions, with nonperturbative hadronization effects absorbed into the latter [10, 11].

For heavy quarkonium systems, the small relative velocity  $v$  of the heavy quark constituents introduces a clear hierarchy of energy scales. The separation between the short-distance scale  $1/m_Q$  and the bound-state formation scale  $1/(m_Q v)$  provides the theoretical foundation for nonrelativistic QCD (NRQCD) [12]. Within this framework, quarkonium production processes can be factorized into short-distance coefficients (SDCs) and long-distance matrix elements (LDMEs), organized as double expansions in  $\alpha_s$  and  $v$  [13].

The fragmentation functions for heavy quarkonium have been extensively studied at leading order (LO) within the NRQCD factorization formalism. Results are available for both gluon and heavy-quark fragmentation into  $S$ -wave and  $P$ -wave quarkonium states, and have been further extended to higher orbital angular momentum channels, including  $D$ -wave states [14–22].

Beyond the LO, QCD corrections to fragmentation functions have been computed for a variety of channels. In particular, next-to-leading-order (NLO) QCD corrections are now available for several  $S$ -wave fragmentation processes and have been applied to both quarkonium and  $B_c$  production [23–28]. Related studies have also investigated the production of higher orbital excitations in hadron colliders [29].

Relativistic corrections constitute another essential ingredient for improving the theoretical accuracy of fragmentation functions. For  $S$ -wave states, relativistic corrections at  $\mathcal{O}(v^2)$  have been systematically studied, and sizable effects have been observed in both quark- and selected gluon-fragmentation channels [30–32]. Higher-order relativistic corrections have been studied in detail, with

complete  $\mathcal{O}(v^4)$  analyses carried out for gluon-fragmentation processes [33] as well as for heavy-quark fragmentation channels [34]. In contrast, relativistic corrections to heavy-quark fragmentation into  $P$ -wave quarkonium remain largely unexplored. Existing studies are limited to LO results, and a complete  $\mathcal{O}(v^2)$  analysis has not yet been carried out for these channels [17, 19].

For systems composed of heavy quarks with unequal masses, such as the  $B_c$  family, relativistic effects are expected to interplay with mass asymmetry, potentially leading to additional modifications of fragmentation dynamics. Although fragmentation functions for  $B_c$  mesons have been studied at LO and at NLO in  $\alpha_s$  [24, 26, 27], a systematic treatment of relativistic corrections for  $P$ -wave  $B_c$  states is still missing.

In this work, we present a systematic analysis of heavy-quark fragmentation into all color-singlet(CS)  $P$ -wave heavy hadrons within the NRQCD factorization framework. After reproducing and confirming the known LO results for heavy-quark fragmentation into  $P$ -wave states [17, 19], we derive the complete  $\mathcal{O}(v^2)$  relativistic corrections to the corresponding fragmentation functions. Our study applies to both equal-mass quarkonium systems and unequal-mass configurations, including the  $B_c$  family. These results close an important gap in the theoretical understanding of  $P$ -wave fragmentation functions and improve the precision of theoretical predictions for  $P$ -wave heavy-hadron production in the large transverse-momentum region.

The remainder of this paper is organized as follows. In Sec. II, we briefly review the gauge-invariant Collins–Soper definition of fragmentation functions. In Sec. III, we introduce the NRQCD factorization framework relevant for heavy-quark fragmentation. In Sec. IV, we present a unified calculation of heavy-quark fragmentation functions into CS  $P$ -wave heavy mesons in the axial gauge, with a formulation that applies to both equal-mass quarkonium systems and unequal-mass configurations, including the  $B_c$  family. In Sec. V, we extract the corresponding SDCs through matching to the NRQCD expansion. In Sec. VI, we provide numerical results and discussions, with particular emphasis on the impact of the  $\mathcal{O}(v^2)$  relativistic corrections for different  $P$ -wave channels. In Sec. VII, we present a comparison between the fragmentation approximation and the full calculation for  $P$ -wave charmonium production. In Sec. VIII, we summarize our main results. In Appendix A, we present the expansion of the squared amplitude for  $P$ -wave relativistic corrections, using the equal-mass case as an explicit example. In Appendices B and C, we list the SDCs for all  $P$ -wave states in the equal-mass and unequal-mass cases, respectively.

## II. Collins–Soper definition of fragmentation functions

To compute the fragmentation functions for heavy-quark fragmentation into  $P$ -wave heavy quarkonium, we adopt the gauge-invariant operator definition proposed by Collins and Soper [10]. The calculation is carried out in the light-cone coordinate system, which allows a transparent separation of longitudinal and transverse degrees of freedom and is therefore convenient for analyzing the kinematic structure of the fragmentation process.

In light-cone coordinates, an arbitrary four-vector  $p^\mu$  is written as

$$p^\mu = (p^+, p^-, \mathbf{p}_T), \quad (1)$$

$$p^+ = (p^0 + p^3)/\sqrt{2}, \quad (2)$$

$$p^- = (p^0 - p^3)/\sqrt{2}. \quad (3)$$

The scalar product of two four-momenta  $p$  and  $q$  is expressed as

$$p \cdot q = p^+ q^- + p^- q^+ - \mathbf{p}_T \cdot \mathbf{q}_T. \quad (4)$$

We introduce a light-cone vector

$$\hat{n}^\mu = (0, 1, \mathbf{0}_T), \quad (5)$$

with  $\hat{n}^2 = 0$ . Based on this, the gauge-invariant fragmentation function for a heavy quark fragmenting

into a quarkonium state  $H$  is defined by Collins and Soper as [10]

$$\begin{aligned}
D_{H/Q}(z) = & \frac{z^{d-3}}{4\pi} \int dx^- e^{-iP^+x^-/z} \frac{1}{3} \text{Tr}_{\text{color}} \frac{1}{2} \text{Tr}_{\text{Dirac}} \\
& \times \left\{ \hat{n} \cdot \gamma \langle 0 | Q(0) \bar{P} \exp \left[ -ig_s \int_0^\infty d\lambda \hat{n} \cdot A^T(\lambda \hat{n}^\mu) \right] \right. \\
& \times a_H^\dagger(P^+, \mathbf{0}_T) a_H(P^+, \mathbf{0}_T) P \exp \left[ ig_s \int_{x^-}^\infty d\lambda \hat{n} \cdot A^T(\lambda \hat{n}^\mu) \right] \\
& \left. \times \bar{Q}(0, x^-, \mathbf{0}_T) | 0 \rangle \right\}. \tag{6}
\end{aligned}$$

In this definition, the longitudinal momentum fraction is given by  $z = \frac{P^+}{k^+}$ , where  $k^+$  denotes the light-cone “+” component of the fragmenting heavy-quark momentum, and  $P^+$  is that of the produced hadron  $H$ . The calculation is performed in  $d = 4 - 2\epsilon$  space-time dimensions using dimensional regularization. Since no ultraviolet or infrared divergences appear in the present analysis, we set  $d = 4$  in the final expressions. The path-ordered exponential,  $P \exp\{\dots\}$ , corresponds to a Wilson line and ensures the gauge invariance of the nonlocal operator. The operator  $a_H^\dagger$  creates the hadronic state  $H$ , and  $A_\mu$  denotes the gluon field.

### III. NRQCD factorization formalism

In the large transverse-momentum region, the production of bound states composed of a heavy quark and a heavy antiquark is dominated by the fragmentation mechanism. According to the QCD factorization theorem, the corresponding differential cross section can be expressed as a convolution of the partonic production cross section and the fragmentation function, a structure that directly follows from QCD factorization [10, 11].

When the final state is a bound system formed by a heavy quark and a heavy antiquark, either of equal or unequal flavors, the presence of the heavy-quark mass scale, which is much larger than  $\Lambda_{\text{QCD}}$ , introduces several well-separated energy scales in the fragmentation process. These include the heavy-quark mass scale  $m$ , the typical relative-momentum scale  $mv$ , and the nonrelativistic kinetic-energy scale  $mv^2$ . In the nonrelativistic limit  $v \ll 1$ , these scales satisfy the hierarchy

$$mv^2 \ll mv \ll m. \tag{7}$$

Exploiting this clear separation of scales, the NRQCD effective field theory integrates out the high-energy degrees of freedom at the scale  $m$ , thereby systematically separating the short-distance production of the heavy quark–antiquark pair from the long-distance nonperturbative dynamics associated with bound-state formation [12, 13]. Within this framework, all nonperturbative effects related to hadronization are absorbed into NRQCD LDMEs, allowing fragmentation functions to be further factorized within the NRQCD formalism.

Accordingly, the fragmentation function for a heavy quark  $Q$  fragmenting into a hadronic state  $H$  can be written as a sum of products of SDCs and the corresponding NRQCD LDMEs

$$D_{H/Q}(z) = \sum_n [F^n(z) \langle 0 | \mathcal{O}^H(n) | 0 \rangle + G^n(z) \langle 0 | \mathcal{P}^H(n) | 0 \rangle] + \mathcal{O}(v^4), \tag{8}$$

where  $F^n(z)$  and  $G^n(z)$  are SDCs that can be calculated perturbatively in QCD. The matrix elements  $\langle 0 | \mathcal{O}^H(n) | 0 \rangle$  and  $\langle 0 | \mathcal{P}^H(n) | 0 \rangle$  denote the NRQCD LDMEs corresponding to the intermediate state  $n$ .

In this work, we focus on the production of  $P$ -wave heavy-quark bound states. Under the leading Fock-state approximation, only CS NRQCD production operators with the same quantum numbers as the hadronic state  $H$  are retained. For  $P$ -wave states, the dominant CS channels include  ${}^1P_1^{[1]}$  and  ${}^3P_J^{[1]}$  with  $J = 0, 1, 2$ . Within the NRQCD factorization framework, relativistic corrections are

described by higher-dimensional NRQCD operators that carry the same quantum numbers and are organized as an expansion in powers of the relative velocity  $v$  of the heavy quarks. The corresponding SDCs share the same dynamical structure as those at LO and can be determined through matching calculations performed for the fragmentation of a free heavy quark–antiquark pair. This procedure allows one to consistently obtain the  $\mathcal{O}(v^2)$  and higher-order relativistic corrections to the production of  $P$ -wave bound states.

Based on the above discussion, the NRQCD production operators corresponding to hadronic states with quantum numbers  ${}^1P_1^{[1]}$  and  ${}^3P_J^{[1]}$  are listed below.

$$\mathcal{O}^H({}^1P_1) = \frac{1}{N_c} \chi^\dagger \left( -\frac{i \overleftrightarrow{\mathbf{D}}}{2} \right) \psi \sum_X |H+X\rangle \langle H+X| \psi^\dagger \left( -\frac{i \overleftrightarrow{\mathbf{D}}}{2} \right) \chi, \quad (9)$$

$$\mathcal{P}^H({}^1P_1) = \frac{1}{2N_c} \left[ \chi^\dagger \left( -\frac{i \overleftrightarrow{\mathbf{D}}}{2} \right) \left( \frac{i \overrightarrow{\mathbf{D}}}{2} \right)^2 \psi \sum_X |H+X\rangle \langle H+X| \psi^\dagger \left( -\frac{i \overleftrightarrow{\mathbf{D}}}{2} \right) \chi + \text{H.c.} \right], \quad (10)$$

$$\mathcal{O}^H({}^3P_0) = \frac{1}{3N_c} \chi^\dagger \left( -\frac{i \overleftrightarrow{\mathbf{D}} \cdot \sigma}{2} \right) \psi \sum_X |H+X\rangle \langle H+X| \psi^\dagger \left( -\frac{i \overleftrightarrow{\mathbf{D}} \cdot \sigma}{2} \right) \chi, \quad (11)$$

$$\mathcal{P}^H({}^3P_0) = \frac{1}{6N_c} \left[ \chi^\dagger \left( -\frac{i \overleftrightarrow{\mathbf{D}} \cdot \sigma}{2} \right) \left( \frac{i \overrightarrow{\mathbf{D}}}{2} \right)^2 \psi \sum_X |H+X\rangle \langle H+X| \psi^\dagger \left( -\frac{i \overleftrightarrow{\mathbf{D}} \cdot \sigma}{2} \right) \chi + \text{H.c.} \right], \quad (12)$$

$$\mathcal{O}^H({}^3P_1) = \frac{1}{2N_c} \chi^\dagger \left( -\frac{i \overleftrightarrow{\mathbf{D}} \times \sigma}{2} \right) \psi \sum_X |H+X\rangle \langle H+X| \psi^\dagger \left( -\frac{i \overleftrightarrow{\mathbf{D}} \times \sigma}{2} \right) \chi, \quad (13)$$

$$\mathcal{P}^H({}^3P_1) = \frac{1}{4N_c} \left[ \chi^\dagger \left( -\frac{i \overleftrightarrow{\mathbf{D}} \times \sigma}{2} \right) \left( \frac{i \overrightarrow{\mathbf{D}}}{2} \right)^2 \psi \sum_X |H+X\rangle \langle H+X| \psi^\dagger \left( -\frac{i \overleftrightarrow{\mathbf{D}} \times \sigma}{2} \right) \chi + \text{H.c.} \right], \quad (14)$$

$$\mathcal{O}^H({}^3P_2) = \frac{1}{N_c} \chi^\dagger \left( -\frac{i \overleftrightarrow{\mathbf{D}}^{(i)\sigma^j}}{2} \right) \psi \sum_X |H+X\rangle \langle H+X| \psi^\dagger \left( -\frac{i \overleftrightarrow{\mathbf{D}}^{(i)\sigma^j}}{2} \right) \chi, \quad (15)$$

$$\mathcal{P}^H({}^3P_2) = \frac{1}{2N_c} \left[ \chi^\dagger \left( -\frac{i \overleftrightarrow{\mathbf{D}}^{(i)\sigma^j}}{2} \right) \left( \frac{i \overrightarrow{\mathbf{D}}}{2} \right)^2 \psi \sum_X |H+X\rangle \langle H+X| \psi^\dagger \left( -\frac{i \overleftrightarrow{\mathbf{D}}^{(i)\sigma^j}}{2} \right) \chi + \text{H.c.} \right]. \quad (16)$$

Here,  $H$  denotes the heavy-quarkonium hadronic state in the final state, and  $X$  represents the additional particles produced in association with  $H$ . The sum  $\sum_X |H+X\rangle \langle H+X|$  corresponds to the completeness relation projecting onto the subspace of final states containing the hadron  $H$ . The number of colors is fixed to  $N_c = 3$ . The fields  $\psi$  and  $\chi$  denote the two-component Pauli spinor fields of the heavy quark and antiquark, respectively, and  $\sigma^i$  ( $i = 1, 2, 3$ ) are the Pauli matrices. The operator  $\mathbf{D}$  stands for the spatial components of the covariant derivative  $D^\mu$ . The combination

$$\overleftrightarrow{\mathbf{D}} \equiv \overrightarrow{\mathbf{D}} - \overleftarrow{\mathbf{D}} \quad (17)$$

is introduced to encode the relative momentum of the heavy quark–antiquark pair in the NRQCD operators.

The SDCs are determined through the standard matching procedure within the NRQCD factorization framework. In the matching, the physical hadronic state  $H$  is replaced by an on-shell free heavy quark–antiquark pair carrying the same overall quantum numbers, which may consist of either equal or unequal flavors. Under this replacement, the NRQCD LDMEs reduce to quantities that can be computed perturbatively, while the SDCs retain information solely from the hard scale and are insensitive to the long-distance bound-state dynamics. Consequently, by computing the fragmentation functions for the free heavy quark–antiquark pair and matching them term by term to the NRQCD operator expansion, the SDCs  $F_n(z)$  and  $G_n(z)$  can be uniquely determined.

## IV. Fragmentation function calculation for $P$ -wave heavy mesons

In this section, we present a unified formulation for the fragmentation of a heavy quark into CS  $P$ -wave heavy mesons within the Collins–Soper operator definition. The framework applies to both equal-mass quarkonium systems and unequal-mass states composed of two different heavy flavors, such as the  $B_c$  family.

The momenta of the heavy quark and antiquark forming the bound state are parameterized in terms of the total momentum  $P$  and the relative momentum  $q$  as [35]

$$p_1 = rP + q, \quad (18)$$

$$p_2 = (1 - r)P - q, \quad (19)$$

where the momentum fraction  $r$  is fixed by the quark masses,

$$r = \frac{E_1}{E_1 + E_2}. \quad (20)$$

In the equal-mass limit  $m_1 = m_2$ , one has  $E_1 = E_2$  and hence  $r = 1/2$ . For a general unequal-mass system, the invariant mass of the  $Q_1\bar{Q}_2$  pair reads

$$P^2 = M^2 = (E_1 + E_2)^2, \quad (21)$$

with

$$E_1 = \sqrt{m_1^2 + \mathbf{q}^2}, \quad (22)$$

$$E_2 = \sqrt{m_2^2 + \mathbf{q}^2}. \quad (23)$$

Here,  $M$  denotes the mass of the charmonium state. In the nonrelativistic limit  $\mathbf{q}^2 \ll m_{1,2}^2$ ,  $M = m_1 + m_2$  and  $P^2 \simeq (m_1 + m_2)^2$ . For the equal-mass case,  $m_1 = m_2 = m$ ,  $E_1 = E_2 = E$ . For the invariant magnitude of  $\mathbf{q}$ , there exists a relation associated with the effective velocity  $v$ ,

$$\mathbf{q} = 2\mu v, \quad (24)$$

where

$$\mu = \frac{m_1 m_2}{m_1 + m_2} \quad (25)$$

is the reduced mass of the heavy quark–antiquark system.

The spin-singlet and spin-triplet covariant projection operators for a general heavy-quark system are given by

$$\Pi_0 = \frac{1}{4\sqrt{2N_c} E_1 E_2 (E_1 + m_1)(E_2 + m_2)} (\not{p}_2 - m_2) \gamma^5 \frac{\not{P} + E_1 + E_2}{E_1 + E_2} (\not{p}_1 + m_1), \quad (26)$$

$$\Pi_1 = \frac{1}{4\sqrt{2N_c} E_1 E_2 (E_1 + m_1)(E_2 + m_2)} (\not{p}_2 - m_2) \gamma^\mu \frac{\not{P} + E_1 + E_2}{E_1 + E_2} (\not{p}_1 + m_1), \quad (27)$$

where  $N_c = 3$  and Dirac spinors are normalized as  $u^\dagger u = v^\dagger v = 1$ . In the equal-mass case, these expressions reduce to the standard projection operators commonly used for quarkonium states.

The fragmentation function for a heavy quark  $Q_1$  fragmenting into a pair of  $Q_1\bar{Q}_2$  with quantum numbers  ${}^{2S+1}P_J$  can be written as

$$D_{(Q_1\bar{Q}_2)/Q_1}^{(2S+1)P_J}(z) = 2(E_1 + E_2) \frac{z}{24\pi} \int \frac{dq_1^+ d^2\mathbf{q}_{1T}}{(2\pi)^3 2q_1^+} 2\pi \delta(k^+ - P^+ - q_1^+) F_c \mathcal{A}_{Q_1 \rightarrow (Q_1\bar{Q}_2)[{}^{2S+1}P_J]}, \quad (28)$$

where  $q_1$  denotes the momentum of the recoiling final-state parton, and the color factor is

$$F_c = \text{Tr}(T^a T^a T^b T^b) = \frac{16}{3}. \quad (29)$$

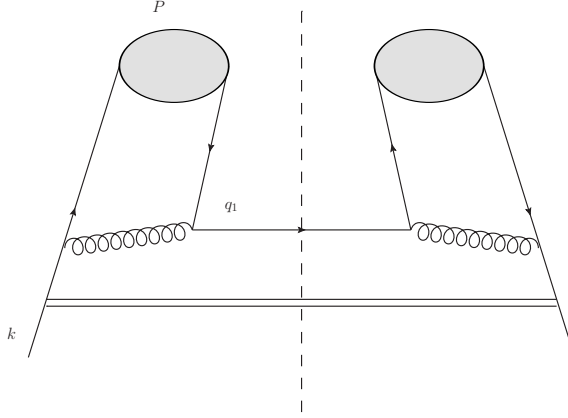


Figure 1: Feynman diagrams for heavy-quark fragmentation into heavy quarkonium at leading-order in  $\alpha_s$ , where the shaded blob denotes the heavy quarkonium state and the double line represents the Wilson line.

The factor  $2(E_1 + E_2)$  originates from the relativistic normalization of the NRQCD heavy-quark pair state. The squared amplitude reads

$$\mathcal{A}_{Q_1 \rightarrow (Q_1 \bar{Q}_2)[^{2S+1}P_J]} = \text{Tr} \left[ \not{q} \mathcal{M}_{P\text{-wave}} (\not{q}_1 + m_2) \mathcal{M}_{P\text{-wave}}^* \right]. \quad (30)$$

Working in the axial gauge  $\hat{n} \cdot A = 0$ , the Wilson line in the Collins–Soper definition vanishes, and the fragmentation function receives contributions only from diagrams involving a single gluon exchange, as shown in Figure 1. The amputated amplitude is given by

$$\mathcal{M}_{P\text{-wave}} = D_{\mu\nu}(l) \frac{\not{P} + \not{q}_1 + m_1}{(P + q_1)^2 - m_1^2} \gamma^\mu \Pi_{0(1)} \gamma^\nu, \quad (31)$$

where  $D_{\mu\nu}(l)$  is the gluon propagator in the axial gauge, with the gluon momentum  $l = p_2 + q_1$ . The gluon propagator in the axial gauge takes the form

$$D_{\mu\nu}(l) = \frac{i}{l^2} \left( -g_{\mu\nu} + \frac{l_\mu \hat{n}_\nu + l_\nu \hat{n}_\mu}{l \cdot \hat{n}} \right). \quad (32)$$

With this velocity counting, the  $P$ -wave amplitude can be systematically expanded in powers of  $\mathbf{q}^2$  (or equivalently  $v^2$ ) as

$$\mathcal{M}_{P\text{-wave}} = \mathcal{M}_{P1} + \mathbf{q}^2 \mathcal{M}_{P3} + \mathcal{O}(\mathbf{q}^4). \quad (33)$$

where  $\mathcal{M}_{P1}$  and  $\mathcal{M}_{P3}$  denote the leading and  $\mathcal{O}(v^2)$  contributions, respectively.

$$\begin{aligned} \mathcal{M}_{P1} &= \epsilon^\alpha(L_z) \frac{\partial \mathcal{M}}{\partial q^\alpha} \Big|_{q \rightarrow 0}, \\ \mathcal{M}_{P3} &= -\frac{1}{5 \times 3!} \epsilon^\alpha(L_z) I_\alpha^{\beta\gamma\delta} \frac{\partial^3 \mathcal{M}}{\partial q^\beta \partial q^\gamma \partial q^\delta} \Big|_{q=0} \end{aligned} \quad (34)$$

where

$$I^{\alpha\beta} = -g^{\alpha\beta} + \frac{P^\alpha P^\beta}{M^2} \quad (35)$$

$$I_\alpha^{\beta\gamma\delta} = I_\alpha^\beta I^\gamma\delta + I_\alpha^\gamma I^\beta\delta + I_\alpha^\delta I^\beta\gamma. \quad (36)$$

We perform the expansion details at the squared amplitude level in Appendix A.

## V. Matching of short-distance coefficients

To extract the SDCs for heavy-quark fragmentation into  $P$ -wave meson states, the perturbative fragmentation functions obtained in the previous section are matched term by term to the NRQCD factorization formula. With standard relativistic normalization, the NRQCD matrix elements for a heavy quark-antiquark pair with quantum numbers  $^{2S+1}P_J$  satisfy the normalization conditions

$$\langle \mathcal{O}^{Q_1\bar{Q}_2}(^1P_1) \rangle = 2(d-1)N_c \mathbf{q}^2, \quad (37)$$

$$\langle \mathcal{O}^{Q_1\bar{Q}_2}(^3P_0) \rangle = 2N_c \mathbf{q}^2, \quad (38)$$

$$\langle \mathcal{O}^{Q_1\bar{Q}_2}(^3P_1) \rangle = 2(d-1)N_c \mathbf{q}^2, \quad (39)$$

$$\langle \mathcal{O}^{Q_1\bar{Q}_2}(^3P_2) \rangle = (d+1)(d-2)N_c \mathbf{q}^2, \quad (40)$$

and

$$\langle \mathcal{P}^{Q_1\bar{Q}_2}(n) \rangle = \mathbf{q}^2 \langle \mathcal{O}^{Q_1\bar{Q}_2}(n) \rangle, \quad n = ^1P_1, ^3P_J \ (J = 0, 1, 2), \quad (41)$$

Substituting these matrix elements into the NRQCD factorization formula, the  $P$ -wave fragmentation function can be expressed as

$$D_{Q_1\bar{Q}_2(^1P_1)/Q_1}(z) = 2(d-1)N_c \left( F^{^1P_1}(z) + \mathbf{q}^2 G^{^1P_1}(z) \right), \quad (42)$$

$$D_{Q_1\bar{Q}_2(^3P_0)/Q_1}(z) = 2N_c \left( F^{^3P_0}(z) + \mathbf{q}^2 G^{^3P_0}(z) \right), \quad (43)$$

$$D_{Q_1\bar{Q}_2(^3P_1)/Q_1}(z) = 2(d-1)N_c \left( F^{^3P_1}(z) + \mathbf{q}^2 G^{^3P_1}(z) \right), \quad (44)$$

$$D_{Q_1\bar{Q}_2(^3P_2)/Q_1}(z) = (d+1)(d-2)N_c \left( F^{^3P_2}(z) + \mathbf{q}^2 G^{^3P_2}(z) \right). \quad (45)$$

where  $F^n(z)$  and  $G^n(z)$  correspond to the LO and NLO SDCs in the  $v$  expansion, respectively. By comparing the above expression term by term with the fragmentation function obtained from perturbative calculations in the previous section, the SDCs for all  $P$ -wave states with quantum numbers  $^{2S+1}P_J$  can be determined.

We present the SDCs for all  $P$ -wave states in both the equal-mass and unequal-mass cases. For completeness, the explicit results for the equal-mass case are collected in Appendix B, while those for the unequal-mass case are presented in Appendix C. Our LO results are in agreement with those obtained by Yuan [17] and Ma [19]. Going beyond the LO, we have systematically computed the  $\mathcal{O}(v^2)$  relativistic corrections to heavy-quark fragmentation into  $P$ -wave states. For the equal-mass quarkonium systems, the  $\mathcal{O}(v^2)$  relativistic corrections presented in Eqs. (B.2), (B.4), (B.6), and (B.8) are new results. For the unequal-mass case, relevant for flavored heavy mesons such as the  $B_c$  family, the corresponding  $\mathcal{O}(v^2)$  corrections given in Eqs. (C.2), (C.4), (C.6), and (C.8) are also obtained for the first time. These results constitute the main contributions of the present work.

## VI. Numerical results and discussion

In this section, based on the analytical expressions of the SDCs obtained in the previous section, we perform a numerical analysis of the  $\mathcal{O}(v^2)$  relativistic effects in the fragmentation processes of various  $P$ -wave heavy hadronic states. The relative values of the LDMEs are given by  $\langle 0|\mathcal{O}^H|0 \rangle : \langle 0|\mathcal{P}^H|0 \rangle = 1 : (2\mu)^2 \langle v^2 \rangle$ .  $\langle v^2 \rangle$  adhere to the velocity power scaling rules and are of the order of  $v^2$  as  $v^2 = \langle v^2 \rangle [1 + \mathcal{O}(v^4)]$ .

The charm- and bottom-quark masses are taken from Ref. [36] as

$$m_c = 1.5 \text{ GeV}, \quad m_b = 4.7 \text{ GeV}. \quad (46)$$

For the equal-mass (quarkonium) case, the relativistic velocity parameter  $v^2$  in the CS channel is estimated using the Gremm-Kapustin relation [37], which is given by

$$v^2 = \frac{M_{Q\bar{Q}} - 2m_Q^{\text{pole}}}{m_Q^{\text{QCD}}}, \quad (47)$$

where  $m_Q^{\text{pole}}$  denotes the pole mass of the heavy quark,  $m_Q^{\text{QCD}}$  is the quark mass parameter appearing in NRQCD, and  $M_{Q\bar{Q}}$  represents the experimental mass of the corresponding heavy quarkonium state. Here we take  $m_Q^{\text{QCD}} = m_Q^{\text{pole}}$ , from which we obtain

$$v_{c\bar{c}}^2 = 0.23, \quad v_{b\bar{b}}^2 = 0.1. \quad (48)$$

It should be emphasized that the value of  $v^2$  extracted from the Gremm–Kapustin relation can only be regarded as an order-of-magnitude estimate, and is subject to sizable theoretical uncertainties. Following the commonly adopted ranges in the literature, we take  $\langle v^2 \rangle_{c\bar{c}}$  in the interval  $0.23 \pm 0.05$  and  $\langle v^2 \rangle_{b\bar{b}}$  in the interval  $0.1 \pm 0.05$ . Based on these inputs, we evaluate the integrated ratios of the  $\mathcal{O}(v^2)$  relativistic corrections to the LO fragmentation functions in Table 1. In addition, we further examine the ratios of the  $\mathcal{O}(v^2)$  relativistic SDCs to their LO counterparts, evaluated in the kinematic limits  $z \rightarrow 0$  and  $z \rightarrow 1$ . These two limits correspond to the soft and forward fragmentation regions, respectively. The corresponding results are summarized in Table 2, and compared with those available in Refs. [31, 34]. To illustrate the overall size of the  $\mathcal{O}(v^2)$  relativistic effects more transparently, we also present the fragmentation functions of  $P$ -wave charmonium and bottomonium states as functions of the momentum fraction  $z$ . Specifically, Figure 2 and Figure 3 show the numerical results for the charmonium and bottomonium systems, respectively.

For the unequal-mass case, taking the  $B_c$  meson system as a representative example, we compute the integrated ratios of the  $\mathcal{O}(v^2)$  relativistic corrections to the LO fragmentation functions in the  ${}^1P_1$  and  ${}^3P_J$  ( $J = 0, 1, 2$ ) channels. The corresponding numerical results are listed in Table 3, which allow for a systematic analysis of relativistic effects in heavy-meson fragmentation processes with unequal quark masses.

Table 1: Ratios of the integrated fragmentation functions. The leading-order fragmentation function is denoted by  $D^{(0)}(z)$ . The fragmentation function from relativistic correction is denoted by  $D^{(2)}(z)$ . For the equal-mass case,  $\langle v^2 \rangle_{c\bar{c}} = 0.23 \pm 0.05$  and  $\langle v^2 \rangle_{b\bar{b}} = 0.1 \pm 0.05$  are used.

	$c \rightarrow h_c({}^1P_1)$	$c \rightarrow \chi_{c0}({}^3P_0)$	$c \rightarrow \chi_{c1}({}^3P_1)$	$c \rightarrow \chi_{c2}({}^3P_2)$
$\frac{\int dz D^{(2)}(z)}{\int dz D^{(0)}(z)}$	$-35.36 \pm 7.69\%$	$-38.71 \pm 8.42\%$	$-36.89 \pm 8.02\%$	$-25.73 \pm 5.59\%$
	$b \rightarrow h_b({}^1P_1)$	$b \rightarrow \chi_{b0}({}^3P_0)$	$b \rightarrow \chi_{b1}({}^3P_1)$	$b \rightarrow \chi_{b2}({}^3P_2)$
$\frac{\int dz D^{(2)}(z)}{\int dz D^{(0)}(z)}$	$-15.37 \pm 7.69\%$	$-16.83 \pm 8.42\%$	$-16.04 \pm 8.02\%$	$-11.19 \pm 5.59\%$

Table 2: Ratios of the  $\mathcal{O}(v^2)$  relativistic short-distance coefficients to the leading-order ones in the equal-mass case, evaluated in the kinematic limits  $z \rightarrow 0$  and  $z \rightarrow 1$ , which correspond to the soft and forward fragmentation regions, respectively. These ratios are defined as  $R_{1,2} = m^2 (G^n/F^n)|_{z \rightarrow 0,1}$ .

	${}^1P_1$	${}^3P_0$	${}^3P_1$	${}^3P_2$
$R_1$	$-\frac{23}{10}$	$-\frac{23}{10}$	$-\frac{21}{10}$	$-\frac{17}{10}$
$R_2$	$\frac{7}{50}$	$-\frac{17}{1570}$	$\frac{7}{85}$	$\frac{167}{320}$

For the equal-mass case, we find that the  $\mathcal{O}(v^2)$  relativistic corrections are negative over most of the momentum-fraction region  $z$ . The relativistic effects are numerically more significant in the charmonium system than in bottomonium, which can be traced back to the larger relative velocity of the heavy quarks in the former. This overall trend is consistent with previous observations in heavy-quark fragmentation into  $S$ -wave quarkonia [31].

A comparison among different angular-momentum channels further shows that, for CS  $P$ -wave states, the relative size of the  $\mathcal{O}(v^2)$  corrections is generally larger than that for the corresponding CS  $S$ -wave channels. This indicates that relativistic effects play a more important role in  $P$ -wave

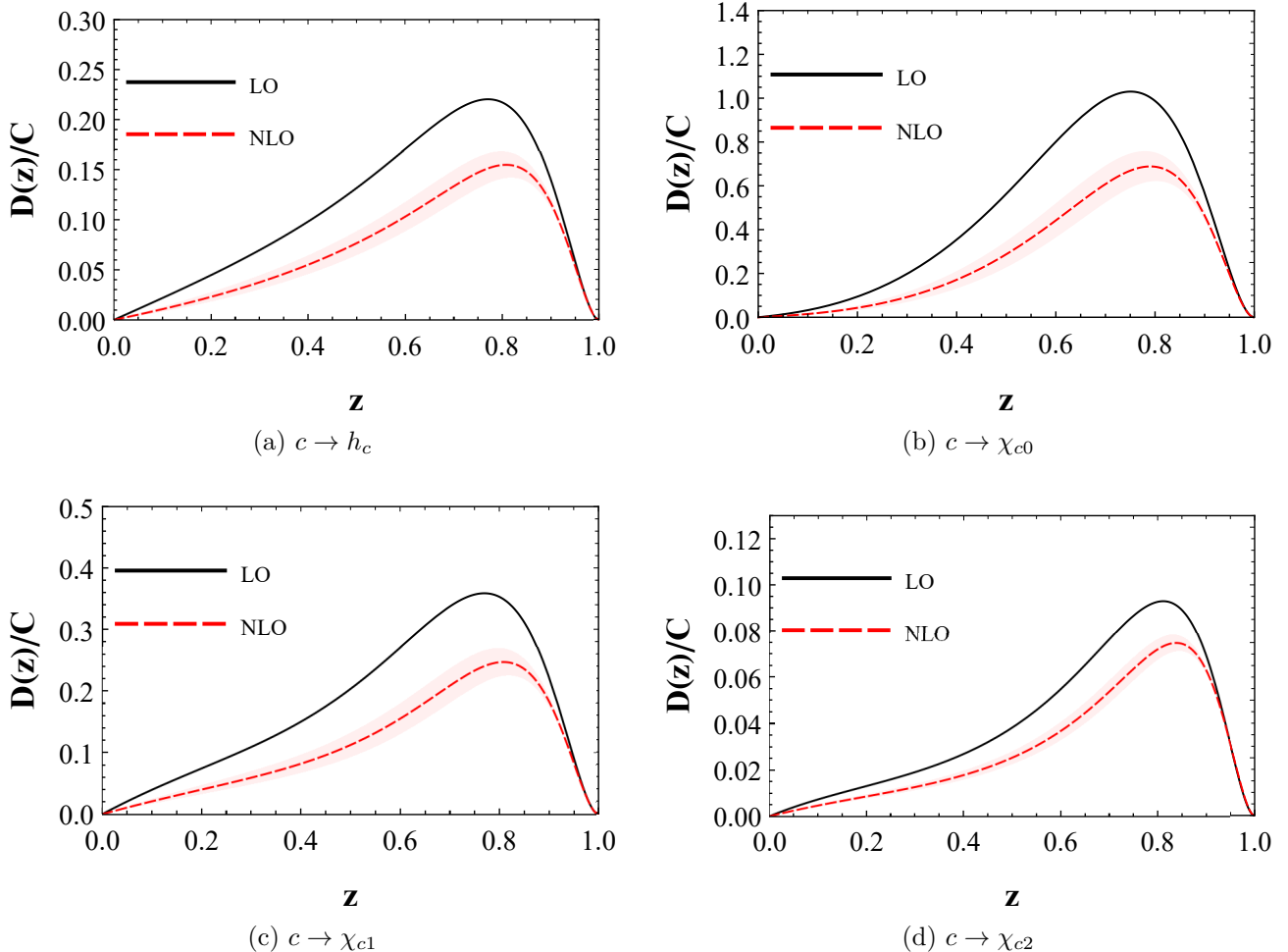


Figure 2: (Color online) The heavy-quark fragmentation functions  $D(c \rightarrow h_c)$ ,  $D(c \rightarrow \chi_{c0})$ ,  $D(c \rightarrow \chi_{c1})$ , and  $D(c \rightarrow \chi_{c2})$  as functions of the momentum fraction  $z$ . The black solid curves denote the leading-order results, while the red dashed curves include the  $\mathcal{O}(v^2)$  relativistic corrections. The shaded bands correspond to the variation of  $\langle v^2 \rangle_{c\bar{c}} = 0.23 \pm 0.05$  in the charmonium system. The charm-quark mass is taken as  $m_c = 1.5$  GeV. The normalization factor is chosen as  $C = 10^{-2} \alpha_s^2 \langle \mathcal{O} \rangle$ .

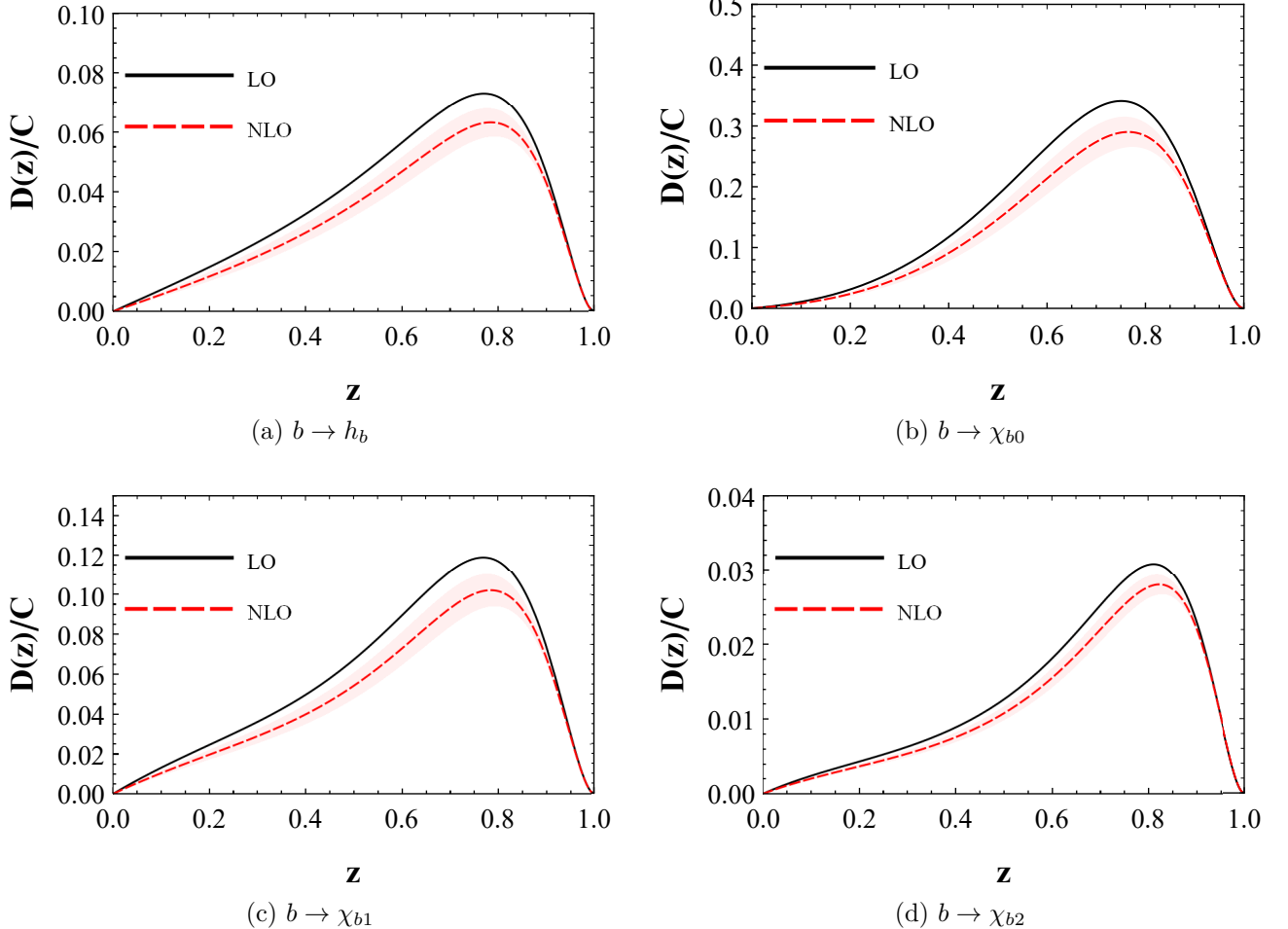


Figure 3: (Color online) The heavy-quark fragmentation functions  $D(b \rightarrow h_b)$ ,  $D(b \rightarrow \chi_{b0})$ ,  $D(b \rightarrow \chi_{b1})$ , and  $D(b \rightarrow \chi_{b2})$  as functions of the momentum fraction  $z$ . The notation and color coding follow those in Figure 2, but with the bottom-quark mass fixed to  $m_b = 4.7$  GeV. The shaded bands correspond to the variation of  $\langle v^2 \rangle_{b\bar{b}} = 0.10 \pm 0.05$  in the bottomonium system. The normalization factor is taken as  $C = 10^{-4} \alpha_s^2 \langle \mathcal{O} \rangle$ .

fragmentation processes. In addition, the numerical results exhibit a strong dependence on the choice of the velocity parameter  $v_{Q\bar{Q}}^2$ , highlighting the sensitivity of the relativistic corrections to the internal dynamics of the bound state.

Noticeable differences are also observed among various  $P$ -wave channels. In particular, the relativistic corrections to the  ${}^3P_2$  state are significantly smaller than those for the  ${}^1P_1$ ,  ${}^3P_0$ , and  ${}^3P_1$  channels. To further quantify the impact of relativistic effects, we evaluate the ratios  $R_i$  ( $i = 1, 2$ ), which measure the contributions of the  $\mathcal{O}(v^2)$  corrections relative to the LO results. These ratios are summarized in Table 2.

By comparing our results with the corresponding  $S$ -wave fragmentation results in Ref. [31,34], we conclude that, for heavy-quark fragmentation into quarkonium, the relativistic corrections in  $P$ -wave channels are generally larger than those in  $S$ -wave channels. This enhancement becomes particularly pronounced in the  $z \rightarrow 1$  forward-fragmentation region, where the  $\mathcal{O}(v^2)$  corrections have a stronger impact on the fragmentation-function distributions. Therefore, relativistic corrections at order  $v^2$  are indispensable for precision theoretical predictions of  $P$ -wave heavy-quarkonium production.

Table 3: Ratios of the integrated  $\mathcal{O}(v^2)$  relativistic corrections to the integrated leading-order fragmentation functions for  $P$ -wave  $B_c$  mesons in the  ${}^1P_1$  and  ${}^3P_J$  ( $J = 0, 1, 2$ ) channels.

$m_1 = 1.5, m_2 = 4.7$				
	$c \rightarrow c\bar{b}({}^1P_1)$	$c \rightarrow c\bar{b}({}^3P_0)$	$c \rightarrow c\bar{b}({}^3P_1)$	$c \rightarrow c\bar{b}({}^3P_2)$
$\frac{\int dz D^{(2)}(z)}{\langle v^2 \rangle \int dz D^{(0)}(z)}$	-1.54	-1.82	-1.61	-0.44
$m_1 = 4.7, m_2 = 1.5$				
	$b \rightarrow b\bar{c}({}^1P_1)$	$b \rightarrow b\bar{c}({}^3P_0)$	$b \rightarrow b\bar{c}({}^3P_1)$	$b \rightarrow b\bar{c}({}^3P_2)$
$\frac{\int dz D^{(2)}(z)}{\langle v^2 \rangle \int dz D^{(0)}(z)}$	-2.97	-2.69	-2.98	-3.01

For the unequal-mass case, we take the  $B_c$  meson as a representative example and evaluate the ratios of the integrated  $\mathcal{O}(v^2)$  relativistic corrections to the integrated LO fragmentation functions for  $P$ -wave  $B_c$  states in the  ${}^1P_1$  and  ${}^3P_J$  ( $J = 0, 1, 2$ ) channels. For the fragmentation process  $c \rightarrow c\bar{b}$ , the relativistic corrections at order  $\mathcal{O}(v^2)$  exhibit a mild dependence on the quantum numbers of the final-state meson. In particular, the contributions for the  ${}^1P_1$ ,  ${}^3P_0$ , and  ${}^3P_1$  channels are found to be of comparable magnitude, while the correction to the  ${}^3P_2$  channel is noticeably smaller than those of the other  $P$ -wave states. In contrast, for the fragmentation process  $b \rightarrow b\bar{c}$ , the relativistic corrections show much weaker sensitivity to the spin and angular-momentum quantum numbers. The  $\mathcal{O}(v^2)$  contributions to the  ${}^1P_1$  and  ${}^3P_J$  ( $J = 0, 1, 2$ ) channels are numerically similar, indicating that relativistic effects in this channel are largely insensitive to the specific  $P$ -wave configuration. These results reflect the interplay between relativistic effects and mass asymmetry in the  $B_c$  system, and highlight qualitative differences between the  $c \rightarrow c\bar{b}$  and  $b \rightarrow b\bar{c}$  fragmentation mechanisms.

## VII. Application and comparison with full fix-order calculations

We apply the obtained fragmentation functions to the inclusive production of  $P$ -wave charmonium (denoted by  $H$ ) in  $e^+e^-$  annihilation via a virtual photon. The representative Feynman diagrams are shown in Figure 4.

Within the fragmentation approximation, the cross sections can be written as

$$\sigma_{\text{frag}}(e^+e^- \rightarrow \gamma^* \rightarrow H + X_{c\bar{c}}) = 2\sigma(e^+e^- \rightarrow c\bar{c}) \int_{\delta}^1 D_{c \rightarrow H}(z) dz, \quad (49)$$

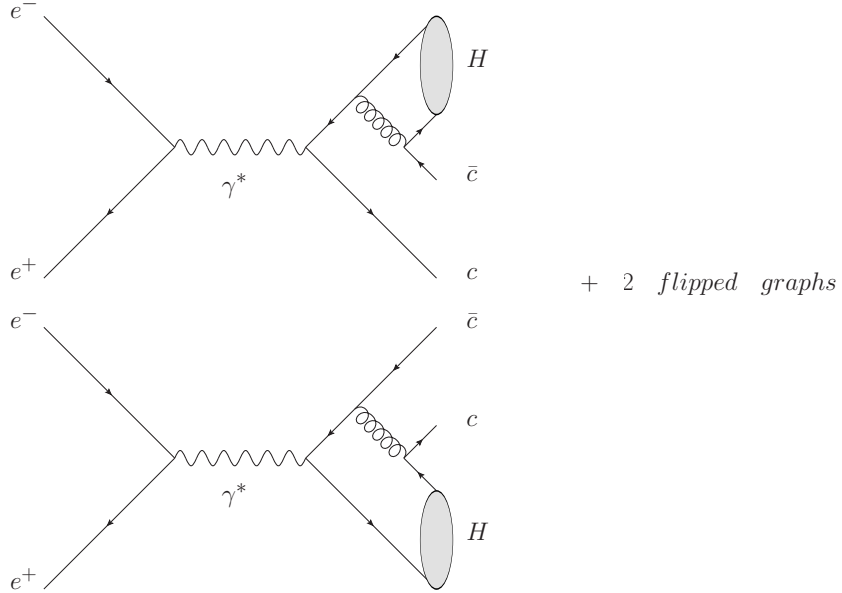


Figure 4: Feynman diagrams for  $e^+ + e^- \rightarrow \gamma^* \rightarrow H + X_{c\bar{c}}$  at quark level.

where  $\sigma(e^+e^- \rightarrow c\bar{c})$  denotes the charm quark pair production cross section,  $D(z)$  is the fragmentation function for a charm quark fragmenting into a  $P$ -wave charmonium state, and  $\delta = 4m_c/E_{\text{cm}}$  where  $E_{\text{cm}}$  is the center-of-mass energy.

Based on the above fragmentation expression, we further plot the ratios between the scattering cross sections of the charmonium production and those of the charm quark pair production as functions of  $E_{\text{cm}}$  as shown in Figure 5. The corresponding ratios of full fixed-order perturbative QCD calculations at LO [38] and up to  $\mathcal{O}(v^2)$  are also plotted in this figure for comparison<sup>1</sup>.

From the Figure 5, one can directly observe that, similar to the LO case [38], the fragmentation and full calculations also remain in good agreement in the high-energy limit for the NLO( $v^2$ ) case. These results provide a twofold validation of both the fragmentation functions and the full NLO( $v^2$ ) calculations to a certain extent. In comparison, there are clear deviations persist at low energies. This implies that the fragmentation function calculations lack accuracy in the low-energy region, where the full NLO calculations need to be employed instead.

## VIII. Summary

In this work, within the framework of NRQCD factorization, we have systematically investigated the  $\mathcal{O}(v^2)$  relativistic corrections to heavy-quark fragmentation into CS  $P$ -wave heavy hadrons, using the Collins–Soper operator definition of fragmentation functions in the axial gauge. Taking the known LO results in Refs. [17, 19] as benchmarks, we reproduce and verify the corresponding LO SDCs. Building upon these benchmarks, we derive analytic expressions for the  $\mathcal{O}(v^2)$  relativistic corrections to heavy-quark fragmentation into the spin-singlet  $^1P_1(h_Q)$  and spin-triplet  $^3P_J(\chi_{QJ}, J = 0, 1, 2)$  states, covering both equal-mass quarkonium systems and unequal-mass configurations. The results presented in this paper provide a systematic extension of the existing fragmentation-function framework for  $P$ -wave heavy hadrons and can be directly applied to precision theoretical predictions for the production of  $h_Q$  and  $\chi_{QJ}$  states at high-energy colliders. We also perform a detailed comparison between the fragmentation-approximation results and the full fixed-order calculation, and find that they become consistent in the high-energy region. Moreover, the present analysis establishes a unified theoretical basis for future studies of higher-order relativistic corrections in heavy-quark fragmentation processes.

<sup>1</sup>In our other recent work, we revisit the relativistic corrections to the inclusive processes  $e^+e^- \rightarrow J/\psi + X_{c\bar{c}}$  and  $e^+e^- \rightarrow J/\psi + X_{\text{non } c\bar{c}}$  at  $B$ -factory energies. We consider the expansions of all the kinematic final-state momenta by relative momentum  $\mathbf{q}$ . The corresponding paper is in preparation [39].

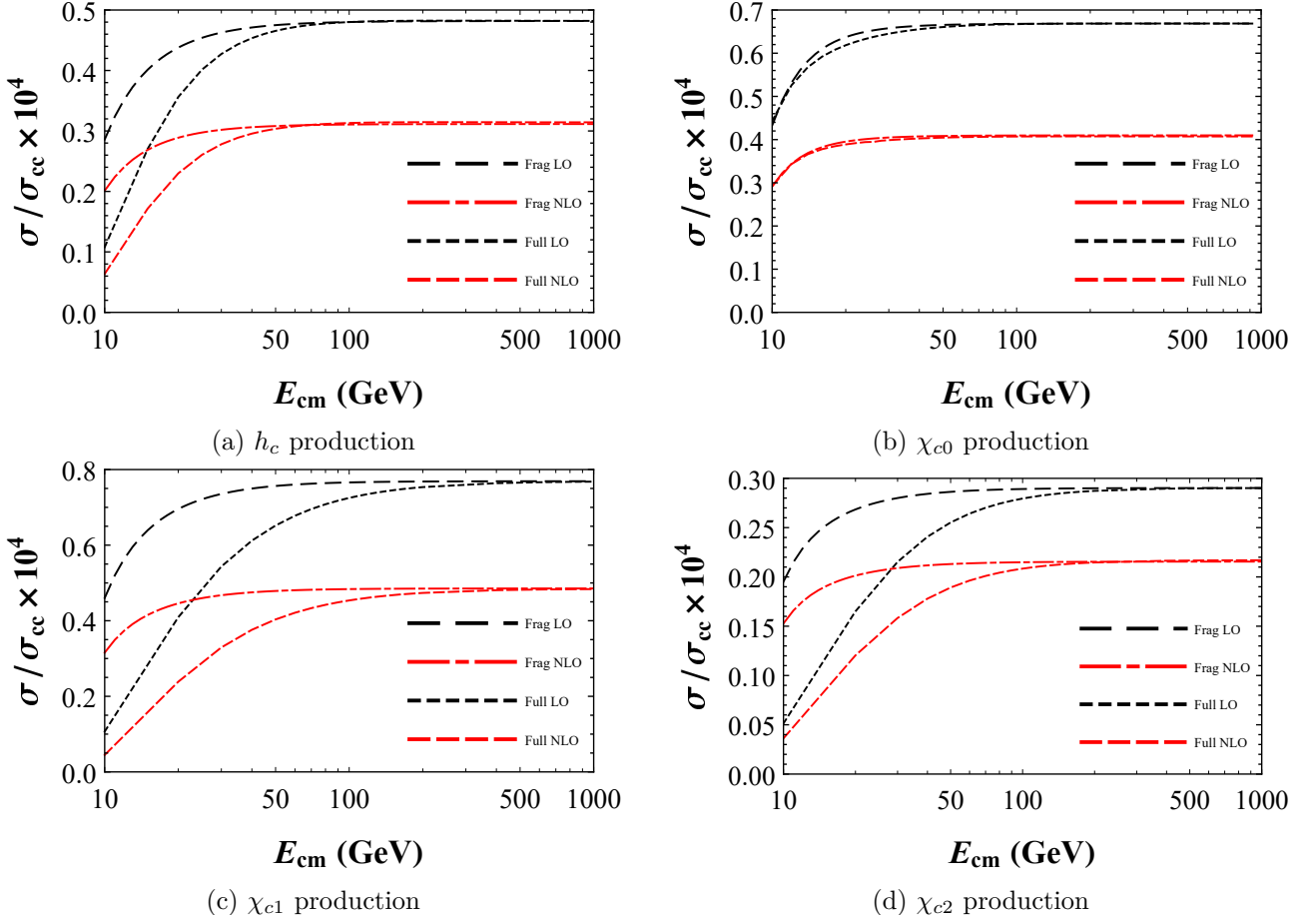


Figure 5: (Color online) Ratios of cross sections  $\sigma(e^+e^- \rightarrow H + X_{c\bar{c}})$  and  $\sigma(e^+e^- \rightarrow c\bar{c})$  as a function of the center-of-mass energy  $E_{\text{cm}}$ . Here, “Frag LO” and “Frag NLO” denote the leading-order and next-to-leading-order results in the fragmentation approximation, while “Full LO” and “Full NLO” denote the leading-order and next-to-leading-order results from the full fixed-order calculation, respectively.

## Acknowledgements

This work was supported by the National Natural Science Foundation of China (No. 11705078, 12575087).

## Appendix

### A. Order-by-order expansion of the squared amplitude for $P$ -wave states

For definiteness, we illustrate the procedure in the equal-mass limit  $m_1 = m_2 = m$  (quarkonium), where  $E(\mathbf{q}) = \sqrt{m^2 + \mathbf{q}^2}$  and  $E(\mathbf{q}) \rightarrow m$  as  $\mathbf{q} \rightarrow \mathbf{0}$ . To organize the velocity expansion, we rewrite the invariant amplitude in Eq. (30) as

$$\mathcal{M}(q) \equiv \widetilde{\mathcal{M}}(q, E(\mathbf{q})), \quad (\text{A.1})$$

treating  $\widetilde{\mathcal{M}}(q, E)$  as a function of two independent variables  $q$  and  $E$ . In the limit  $q \rightarrow 0$ , one has  $E(\mathbf{q}) \rightarrow m$ . For the  $P$ -wave channel,  $\mathcal{M}(q)$  is odd in  $q$  and hence  $\widetilde{\mathcal{M}}(0, m) = 0$ .

The relativistic dispersion relation is expanded as

$$E(\mathbf{q}) = m + \frac{\mathbf{q}^2}{2m} + \mathcal{O}\left(\frac{\mathbf{q}^4}{m^3}\right). \quad (\text{A.2})$$

Following Eq. (33), the  $P$ -wave component of the squared amplitude, with trace evaluations and other intermediate steps suppressed, can be expanded up to  $\mathcal{O}(v^2)$  as

$$\begin{aligned} |\mathcal{M}_P|^2 = \mathbf{q}^2 & \left\{ \epsilon^\alpha(L_z) \epsilon^{*\alpha'}(L_z) \left[ \frac{\partial \widetilde{\mathcal{M}}}{\partial q^\alpha}(0, m) \frac{\partial \widetilde{\mathcal{M}}^*}{\partial q^{\alpha'}}(0, m) \right] \right\} \\ & - \frac{\mathbf{q}^4}{30} \left\{ \epsilon^\alpha(L_z) \epsilon^{*\alpha'}(L_z) I_{\alpha'}^{\beta\gamma\delta} \left[ \frac{\partial \widetilde{\mathcal{M}}}{\partial q^\alpha}(0, m) \frac{\partial^3 \widetilde{\mathcal{M}}^*}{\partial q^\beta \partial q^\gamma \partial q^\delta}(0, m) + \text{H.c.} \right] \right\} \\ & + \frac{\mathbf{q}^4}{2m} \frac{\partial}{\partial E} \left\{ \epsilon^\alpha(L_z) \epsilon^{*\alpha'}(L_z) \left[ \frac{\partial \widetilde{\mathcal{M}}}{\partial q^\alpha}(0, E) \frac{\partial \widetilde{\mathcal{M}}^*}{\partial q^{\alpha'}}(0, E) \right] \right\} + \mathcal{O}(v^4). \end{aligned} \quad (\text{A.3})$$

For the spin-triplet  ${}^3P_J$  states ( $J = 0, 1, 2$ ), the physical polarization degrees of freedom arise from the coupling of the orbital and spin polarizations. By combining the orbital angular momentum  $L = 1$  and the spin  $S = 1$ , the total angular-momentum polarization tensors can be defined as

$$\sum_{L_z, S_z} \epsilon^\alpha(L_z) \epsilon^\mu(S_z) \langle 1L_z; 1S_z | JJ_z \rangle = \epsilon_{(J)}^{\alpha\mu}(J_z), \quad (\text{A.4})$$

where  $\langle 1L_z; 1S_z | JJ_z \rangle$  denotes the Clebsch–Gordan coefficient for coupling orbital angular momentum  $L = 1$  and spin  $S = 1$  to form a state with total angular momentum  $J$ . The polarization sum relations for the  ${}^3P_J$  states are given by

$$\sum_{J_z} \epsilon_{(0)}^{\alpha\mu}(J_z) \epsilon_{(0)}^{*\alpha'\mu'}(J_z) = \frac{1}{d-1} I^{\alpha\mu} I^{\alpha'\mu'}, \quad (\text{A.5})$$

$$\sum_{J_z} \epsilon_{(1)}^{\alpha\mu}(J_z) \epsilon_{(1)}^{*\alpha'\mu'}(J_z) = \frac{1}{2} \left( I^{\alpha\alpha'} I^{\mu\mu'} - I^{\alpha\mu'} I^{\alpha'\mu} \right), \quad (\text{A.6})$$

$$\sum_{J_z} \epsilon_{(2)}^{\alpha\mu}(J_z) \epsilon_{(2)}^{*\alpha'\mu'}(J_z) = \frac{1}{2} \left( I^{\alpha\alpha'} I^{\mu\mu'} + I^{\alpha\mu'} I^{\alpha'\mu} \right) - \frac{1}{d-1} I^{\alpha\mu} I^{\alpha'\mu'}. \quad (\text{A.7})$$

## B. Short-distance coefficients for $P$ -wave states in the equal-mass case

For the  ${}^1P_1$ , we have

$$F^{{}^1P_1}(z) = \frac{16\alpha_s^2 z(z-1)^2}{243m^5(z-2)^8} \times (9z^6 - 56z^5 + 140z^4 - 160z^3 + 176z^2 - 128z + 64), \quad (\text{B.1})$$

$$G^{{}^1P_1}(z) = -\frac{8\alpha_s^2 z(1-z)^2}{18225m^7(2-z)^{10}} \times (3675z^8 - 39844z^7 + 169032z^6 - 373552z^5 + 483904z^4 - 535360z^3 + 498560z^2 - 295680z + 88320), \quad (\text{B.2})$$

For the  ${}^3P_0$ , we have

$$F^{{}^3P_0}(z) = \frac{16\alpha_s^2 z(z-1)^2}{729m^5(z-2)^8} \times (59z^6 - 376z^5 + 1060z^4 - 1376z^3 + 528z^2 + 384z + 192), \quad (\text{B.3})$$

$$G^{{}^3P_0}(z) = -\frac{8\alpha_s^2 z(1-z)^2}{18225m^7(2-z)^{10}} \times (7035z^8 - 80404z^7 + 375432z^6 - 967792z^5 + 1397824z^4 - 961600z^3 + 22400z^2 + 119040z + 88320), \quad (\text{B.4})$$

For the  ${}^3P_1$ , we have

$$F^{{}^3P_1}(z) = \frac{64\alpha_s^2 z(z-1)^2}{729m^5(z-2)^8} \times (7z^6 - 54z^5 + 202z^4 - 408z^3 + 496z^2 - 288z + 96), \quad (\text{B.5})$$

$$G^{{}^3P_1}(z) = -\frac{64\alpha_s^2 z(1-z)^2}{18225m^7(2-z)^{10}} \times (515z^8 - 6393z^7 + 33789z^6 - 103684z^5 + 200068z^4 - 254240z^3 + 196080z^2 - 86400z + 20160), \quad (\text{B.6})$$

For the  ${}^3P_2$ , we have

$$F^{{}^3P_2}(z) = \frac{128\alpha_s^2 z(z-1)^2}{3645m^5(z-2)^8} \times (23z^6 - 184z^5 + 541z^4 - 668z^3 + 480z^2 - 192z + 48), \quad (\text{B.7})$$

$$G^{{}^3P_2}(z) = -\frac{32\alpha_s^2 z(1-z)^2}{18225m^7(2-z)^{10}} \times (1593z^8 - 19924z^7 + 99054z^6 - 249760z^5 + 337240z^4 - 267424z^3 + 130976z^2 - 38784z + 6528). \quad (\text{B.8})$$

### C. Short-distance coefficients for $P$ -wave states in the unequal-mass case

For the  ${}^1P_1$ , we have

$$\begin{aligned}
F^{{}^1P_1}(z) = & -\frac{2\alpha_s^2 z(z-1)^2}{729M^5(y_1-1)^3y_1^2(y_1z-1)^8} \\
& \times \left[ (46y_1^6 - 78y_1^5 + 41y_1^4) z^6 \right. \\
& + (24y_1^6 - 240y_1^5 + 318y_1^4 - 144y_1^3) z^5 \\
& + (32y_1^6 - 128y_1^5 + 514y_1^4 - 544y_1^3 + 210y_1^2) z^4 \\
& + (32y_1^5 - 224y_1^4 + 96y_1^3 + 56y_1^2 - 56y_1) z^3 \\
& + (32y_1^4 - 32y_1^3 + 154y_1^2 - 130y_1 + 45) z^2 \\
& + (-24y_1^2 - 6) z \\
& \left. + 6 \right], \tag{C.1}
\end{aligned}$$

$$\begin{aligned}
G^{{}^1P_1}(z) = & \frac{\alpha_s^2 z(1-z)^2}{36450M^7(y_1-1)^5y_1^4(y_1z-1)^{10}} \\
& \times \left[ (-2300y_1^{11} + 19750y_1^{10} - 50040y_1^9 + 62025y_1^8 - 37780y_1^7 + 9395y_1^6) z^8 \right. \\
& + (-1200y_1^{11} + 25120y_1^{10} - 142440y_1^9 + 309154y_1^8 - 355822y_1^7 + 209282y_1^6 - 51174y_1^5) z^7 \\
& + (-1600y_1^{11} + 20160y_1^{10} - 121200y_1^9 + 443628y_1^8 - 799484y_1^7 + 834909y_1^6 - 465468y_1^5 + 110265y_1^4) z^6 \\
& + (1600y_1^{10} - 6480y_1^9 + 36112y_1^8 - 283976y_1^7 + 614186y_1^6 - 725772y_1^5 + 434490y_1^4 - 107540y_1^3) z^5 \\
& + (-22464y_1^8 + 130792y_1^7 - 158992y_1^6 + 81244y_1^5 + 87965y_1^4 - 114220y_1^3 + 38725y_1^2) z^4 \\
& + (1600y_1^8 - 13680y_1^7 + 50560y_1^6 - 200120y_1^5 + 277350y_1^4 - 236830y_1^3 + 112070y_1^2 - 24550y_1) z^3 \\
& + (-1600y_1^7 + 960y_1^6 + 13360y_1^5 + 3460y_1^4 - 5540y_1^3 + 12315y_1^2 - 8900y_1 + 3375) z^2 \\
& + (1200y_1^5 - 3120y_1^4 - 5400y_1^3 + 4110y_1^2 - 1800y_1 - 450) z \\
& \left. - 300y_1^3 + 1530y_1^2 - 900y_1 + 450 \right], \tag{C.2}
\end{aligned}$$

For the  ${}^3P_0$ , we have

$$\begin{aligned}
F^{{}^3P_0}(z) = & -\frac{2\alpha_s^2(z-1)^2z}{729M^5(y_1-1)^3y_1^2(y_1z-1)^8} \\
& \times \left[ (96y_1^8 - 144y_1^7 - 10y_1^6 + 34y_1^5 + 27y_1^4) z^6 \right. \\
& + (-480y_1^7 + 888y_1^6 - 248y_1^5 - 130y_1^4 - 48y_1^3) z^5 \\
& + (832y_1^6 - 1776y_1^5 + 1074y_1^4 - 232y_1^3 + 150y_1^2) z^4 \\
& + (-800y_1^5 + 1728y_1^4 - 1328y_1^3 + 496y_1^2 - 168y_1) z^3 \\
& + (832y_1^4 - 1872y_1^3 + 1682y_1^2 - 714y_1 + 135) z^2 \\
& + (-480y_1^3 + 936y_1^2 - 648y_1 + 162) z \\
& \left. + 96y_1^2 - 144y_1 + 54 \right], \tag{C.3}
\end{aligned}$$

$$\begin{aligned}
G^{{}^3P_0}(z) = & -\frac{\alpha_s^2(z-1)^2z}{36450M^7(y_1-1)^5y_1^4(y_1z-1)^{10}} \\
& \times \left[ (4800y_1^{13} - 29760y_1^{12} + 56380y_1^{11} - 38910y_1^{10} + 2940y_1^9 + 2705y_1^8 + 6560y_1^7 - 4985y_1^6) z^8 \right. \\
& + (-33600y_1^{12} + 210960y_1^{11} - 448080y_1^{10} + 418800y_1^9 - 154154y_1^8 - 3278y_1^7 - 6842y_1^6 + 18354y_1^5) z^7 \\
& + (94400y_1^{11} - 572800y_1^{10} + 1301120y_1^9 - 1515348y_1^8 + 984384y_1^7 - 352879y_1^6 + 98648y_1^5 - 45355y_1^4) z^6 \\
& + (-147200y_1^{10} + 844720y_1^9 - 1930912y_1^8 + 2532736y_1^7 - 2122226y_1^6 + 1125452y_1^5 - 379970y_1^4 + 94140y_1^3) z^5 \\
& + (163200y_1^9 - 985536y_1^8 + 2321288y_1^7 - 3199208y_1^6 + 2853776y_1^5 - 1613175y_1^4 + 540880y_1^3 - 104175y_1^2) z^4 \\
& + (-147200y_1^8 + 991120y_1^7 - 2469200y_1^6 + 3470000y_1^5 - 3032510y_1^4 + 1633810y_1^3 - 499150y_1^2 + 73650y_1) z^3 \\
& + (94400y_1^7 - 592000y_1^6 + 1336000y_1^5 - 1653820y_1^4 + 1232560y_1^3 - 541625y_1^2 + 123000y_1 - 10125) z^2 \\
& + (-33600y_1^6 + 174960y_1^5 - 325440y_1^4 + 334560y_1^3 - 210150y_1^2 + 75600y_1 - 12150) z \\
& \left. + 4800y_1^5 - 20160y_1^4 + 29820y_1^3 - 26250y_1^2 + 15300y_1 - 4050 \right], \tag{C.4}
\end{aligned}$$

For the  ${}^3P_1$ , we have

$$\begin{aligned}
F^{{}^3P_1}(z) = & -\frac{4\alpha_s^2(z-1)^2z}{729M^5(y_1-1)^3y_1^2(y_1z-1)^8} \\
& \times \left[ (12y_1^6 - 26y_1^5 + 17y_1^4) z^6 \right. \\
& + (-16y_1^6 + 46y_1^4 - 48y_1^3) z^5 \\
& + (16y_1^6 - 32y_1^5 + 94y_1^4 - 120y_1^3 + 90y_1^2) z^4 \\
& + (16y_1^5 - 80y_1^4 + 40y_1^3 + 8y_1^2 - 56y_1) z^3 \\
& + (16y_1^4 - 64y_1^3 + 160y_1^2 - 94y_1 + 45) z^2 \\
& \left. + (-24y_1 - 6)z + 6 \right], \tag{C.5}
\end{aligned}$$

$$\begin{aligned}
G^{{}^3P_1}(z) = & \frac{\alpha_s^2(z-1)^2z}{18225M^7(y_1-1)^5y_1^4(y_1z-1)^{10}} \\
& \times \left[ (-600y_1^{11} + 5440y_1^{10} - 15040y_1^9 + 19955y_1^8 - 13020y_1^7 + 3595y_1^6) z^8 \right. \\
& + (800y_1^{11} - 4480y_1^{10} - 4460y_1^9 + 39562y_1^8 - 71946y_1^7 + 55266y_1^6 - 17382y_1^5) z^7 \\
& + (-800y_1^{11} + 5680y_1^{10} - 15060y_1^9 + 54914y_1^8 - 122372y_1^7 + 169427y_1^6 - 121124y_1^5 + 38905y_1^4) z^6 \\
& + (800y_1^{10} - 240y_1^9 - 4664y_1^8 - 48728y_1^7 + 141698y_1^6 - 209556y_1^5 + 150650y_1^4 - 50420y_1^3) z^5 \\
& + (-7232y_1^8 + 25156y_1^7 + 18414y_1^6 - 75068y_1^5 + 124755y_1^4 - 93700y_1^3 + 35725y_1^2) z^4 \\
& + (800y_1^8 - 13840y_1^7 + 76720y_1^6 - 221100y_1^5 + 275870y_1^4 - 212970y_1^3 + 93990y_1^2 - 24550y_1) z^3 \\
& + (-800y_1^7 + 4080y_1^6 - 14060y_1^5 + 42670y_1^4 - 35580y_1^3 + 21605y_1^2 - 7100y_1 + 3375) z^2 \\
& + (1800y_1^4 - 9840y_1^3 + 6870y_1^2 - 3000y_1 - 450) z \\
& \left. - 300y_1^3 + 1410y_1^2 - 900y_1 + 450 \right], \tag{C.6}
\end{aligned}$$

For the  ${}^3P_2$ , we have

$$\begin{aligned}
F^{{}^3P_2}(z) = & -\frac{8\alpha_s^2(z-1)^2z}{3645M^5(y_1-1)^3(y_1z-1)^8} \\
& \times \left[ (12y_1^6 - 36y_1^5 + 91y_1^4 - 112y_1^3 + 60y_1^2) z^6 \right. \\
& + (-24y_1^5 + 132y_1^4 - 412y_1^3 + 472y_1^2 - 240y_1) z^5 \\
& + (92y_1^4 - 336y_1^3 + 702y_1^2 - 608y_1 + 300) z^4 \\
& + (-40y_1^3 - 96y_1^2 + 188y_1 - 232) z^3 \\
& + (92y_1^2 - 108y_1 + 151) z^2 \\
& + (-24y_1 - 36) z \\
& \left. + 12 \right], \tag{C.7}
\end{aligned}$$

$$\begin{aligned}
G^{{}^3P_2}(z) = & \frac{2\alpha_s^2(z-1)^2z}{18225M^7(y_1-1)^5y_1^2(y_1z-1)^{10}} \\
& \times \left[ (-120y_1^{11} + 1068y_1^{10} - 3970y_1^9 + 11025y_1^8 - 19290y_1^7 + 20179y_1^6 - 11432y_1^5 + 2900y_1^4) z^8 \right. \\
& + (480y_1^{10} - 4296y_1^9 + 20376y_1^8 - 64134y_1^7 + 113144y_1^6 - 117034y_1^5 + 65912y_1^4 - 16896y_1^3) z^7 \\
& + (-1520y_1^9 + 14224y_1^8 - 59678y_1^7 + 158799y_1^6 - 248022y_1^5 + 242893y_1^4 - 134960y_1^3 + 35680y_1^2) z^6 \\
& + (2480y_1^8 - 18832y_1^7 + 52804y_1^6 - 107980y_1^5 + 141836y_1^4 - 143588y_1^3 + 88592y_1^2 - 28560y_1) z^5 \\
& + (-2640y_1^7 + 14016y_1^6 - 6038y_1^5 - 29101y_1^4 + 81466y_1^3 - 69027y_1^2 + 25304y_1 + 1500) z^4 \\
& + (2480y_1^6 - 15952y_1^5 + 27632y_1^4 - 45830y_1^3 + 35408y_1^2 - 14818y_1 - 1160) z^3 \\
& + (-1520y_1^5 + 6304y_1^4 + 494y_1^3 - 2783y_1^2 + 3158y_1 + 755) z^2 \\
& + (480y_1^4 - 2376y_1^3 + 756y_1^2 - 696y_1 - 180) z \\
& \left. - 120y_1^3 + 468y_1^2 - 120y_1 + 60 \right]. \tag{C.8}
\end{aligned}$$

## References

- [1] N. Brambilla, S. Eidelman, B. K. Heltsley, R. Vogt, G. T. Bodwin, E. Eichten, A. D. Frawley, A. B. Meyer, R. E. Mitchell and V. Papadimitriou, *et al.* “Heavy Quarkonium: Progress, Puzzles, and Opportunities,” *Eur. Phys. J. C* **71**, 1534 (2011) doi:10.1140/epjc/s10052-010-1534-9 [arXiv:1010.5827 [hep-ph]].
- [2] Z. B. Kang, J. W. Qiu and G. Sterman, “Heavy quarkonium production at colliders energies: factorization and evolution,” *Phys. Rev. Lett.* **108**, 102002 (2012) doi:10.1103/PhysRevLett.108.102002 [arXiv:1109.1520 [hep-ph]].
- [3] B. Gong, X. Q. Li and J. X. Wang, “QCD corrections to  $J/\psi$  production via color-octet states at Tevatron and LHC,” *Phys. Lett. B* **673**, 197–200 (2009) [erratum: *Phys. Lett. B* **693**, 612–613 (2010)] doi:10.1016/j.physletb.2009.02.026 [arXiv:0805.4751 [hep-ph]].
- [4] Y. Q. Ma, Y. J. Zhang and K. T. Chao, “QCD correction to  $e^+e^- \rightarrow J/\psi + gg$  at B Factories,” *Phys. Rev. Lett.* **102**, 162002 (2009) doi:10.1103/PhysRevLett.102.162002 [arXiv:0812.5106 [hep-ph]].
- [5] Y. J. Zhang, Y. Q. Ma, K. Wang and K. T. Chao, “QCD radiative correction to color-octet  $J/\psi$  inclusive production at B Factories,” *Phys. Rev. D* **81**, 034015 (2010) doi:10.1103/PhysRevD.81.034015 [arXiv:0911.2166 [hep-ph]].
- [6] Z. G. He, Y. Fan and K. T. Chao, “Relativistic correction to  $e^+e^- \rightarrow J/\psi + gg$  at B factories and constraint on color-octet matrix elements,” *Phys. Rev. D* **81**, 054036 (2010) doi:10.1103/PhysRevD.81.054036 [arXiv:0910.3636 [hep-ph]].

- [7] G. Z. Xu, Y. J. Li, K. Y. Liu and Y. J. Zhang, “Relativistic Correction to Color Octet  $J/\psi$  Production at Hadron Colliders,” Phys. Rev. D **86**, 094017 (2012) doi:10.1103/PhysRevD.86.094017 [arXiv:1203.0207 [hep-ph]].
- [8] Y. J. Li, G. Z. Xu, K. Y. Liu and Y. J. Zhang, “Relativistic Correction to  $J/\psi$  and  $\Upsilon$  Pair Production,” JHEP **07**, 051 (2013) doi:10.1007/JHEP07(2013)051 [arXiv:1303.1383 [hep-ph]].
- [9] G. Z. Xu, Y. J. Li, K. Y. Liu and Y. J. Zhang, “ $\alpha_s v^2$  corrections to  $\eta_c$  and  $\chi_{cJ}$  production recoiled with a photon at  $e^+e^-$  colliders,” JHEP **10**, 071 (2014) doi:10.1007/JHEP10(2014)071 [arXiv:1407.3783 [hep-ph]].
- [10] J. C. Collins and D. E. Soper, “Parton Distribution and Decay Functions,” Nucl. Phys. B **194**, 445–492 (1982) doi:10.1016/0550-3213(82)90021-9.
- [11] J. C. Collins, D. E. Soper and G. Sterman, “Perturbative Quantum Chromodynamics,” World Scientific, Singapore (1989).
- [12] W. E. Caswell and G. P. Lepage, “Effective Lagrangians for bound state problems in QED, QCD, and other field theories,” Phys. Lett. B **167**, 437–442 (1986) doi:10.1016/0370-2693(86)91297-9.
- [13] G. T. Bodwin, E. Braaten and G. P. Lepage, “Rigorous QCD analysis of inclusive annihilation and production of heavy quarkonium,” Phys. Rev. D **51**, 1125–1171 (1995) doi:10.1103/PhysRevD.51.1125.
- [14] E. Braaten and T. C. Yuan, “Gluon fragmentation into heavy quarkonium,” Phys. Rev. Lett. **71**, 1673 (1993) doi:10.1103/PhysRevLett.71.1673.
- [15] E. Braaten, K. m. Cheung and T. C. Yuan, “Z0 decay into charmonium via charm quark fragmentation,” Phys. Rev. D **48**, 4230–4235 (1993) doi:10.1103/PhysRevD.48.4230.
- [16] E. Braaten and T. C. Yuan, “Gluon fragmentation into P wave heavy quarkonium,” Phys. Rev. D **50**, 3176–3180 (1994) doi:10.1103/PhysRevD.50.3176.
- [17] T. C. Yuan, “Perturbative QCD fragmentation functions for production of P wave mesons with charm and beauty,” Phys. Rev. D **50**, 5664–5675 (1994) doi:10.1103/PhysRevD.50.5664.
- [18] J. P. Ma, “Gluon fragmentation into P wave triplet quarkonium,” Nucl. Phys. B **447**, 405–424 (1995) doi:10.1016/0550-3213(95)00270-3.
- [19] J. P. Ma, “Quark fragmentation into P wave triplet quarkonium,” Phys. Rev. D **53**, 1185–1190 (1996) doi:10.1103/PhysRevD.53.1185.
- [20] P. L. Cho and M. B. Wise, “Gluon fragmentation to D wave quarkonia,” Phys. Rev. D **51**, 3352–3356 (1995) doi:10.1103/PhysRevD.51.3352.
- [21] C. f. Qiao, F. Yuan and K. T. Chao, “Gluon fragmentation to D wave triplet quarkonia,” Phys. Rev. D **55**, 5437–5444 (1997) doi:10.1103/PhysRevD.55.5437.
- [22] K. m. Cheung and T. C. Yuan, “Heavy quark fragmentation functions for D-wave quarkonium and charmed beauty mesons,” Phys. Rev. D **53**, 3591–3603 (1996) doi:10.1103/PhysRevD.53.3591.
- [23] P. Zhang, C. Y. Wang, X. Liu, Y. Q. Ma, C. Meng and K. T. Chao, “Semi-analytical calculation of gluon fragmentation into  $^1S_0^{[1,8]}$  quarkonia at NLO,” JHEP **04**, 116 (2019) doi:10.1007/JHEP04(2019)116.
- [24] X. C. Zheng, C. H. Chang, T. F. Feng and X. G. Wu, “QCD NLO fragmentation functions for  $c$  or  $\bar{b}$  quark to  $B_c$  or  $B_c^*$  meson and their application,” Phys. Rev. D **100**, 034004 (2019) doi:10.1103/PhysRevD.100.034004.

[25] F. Feng and Y. Jia, “Next-to-leading-order QCD corrections to gluon fragmentation into quarkonia,” Chin. Phys. C **47**, 033103 (2023) doi:10.1088/1674-1137/ac1aa.

[26] X. C. Zheng, C. H. Chang and X. G. Wu, “Fragmentation functions for gluon into  $B_c$  or  $B_c^*$  meson,” JHEP **05**, 036 (2022) doi:10.1007/JHEP05(2022)036.

[27] F. Feng, Y. Jia and D. Yang, “Gluon fragmentation into  $B_c^{(*)}$  in NRQCD factorization,” Phys. Rev. D **106**, 054030 (2022) doi:10.1103/PhysRevD.106.054030.

[28] Z. Y. Zhang, X. C. Zheng and X. G. Wu, “Production of the  $B_c$  meson at the CEPC,” Eur. Phys. J. C **82**, 246 (2022) doi:10.1140/epjc/s10052-022-10212-4.

[29] A. V. Berezhnoy, I. N. Belov and A. K. Likhoded, “Production of D-wave states of  $\bar{b}c$  quarkonium at the LHC,” Phys. Rev. D **103**, 114001 (2021) doi:10.1103/PhysRevD.103.114001.

[30] G. T. Bodwin and J. Lee, “Relativistic corrections to gluon fragmentation into spin-triplet S-wave quarkonium,” Phys. Rev. D **69**, 054003 (2004) doi:10.1103/PhysRevD.69.054003.

[31] W. L. Sang, L. F. Yang and Y. Q. Chen, “Relativistic corrections to heavy quark fragmentation to S-wave heavy mesons,” Phys. Rev. D **80**, 014013 (2009) doi:10.1103/PhysRevD.80.014013.

[32] X. G. Gao, Y. Jia, L. Li and X. Xiong, “Relativistic correction to gluon fragmentation into pseudoscalar quarkonium,” Chin. Phys. C **41**, 023103 (2017) doi:10.1088/1674-1137/41/2/023103.

[33] G. T. Bodwin, U. R. Kim and J. Lee, “Higher-order relativistic corrections to gluon fragmentation into spin-triplet S-wave quarkonium,” JHEP **11**, 020 (2012) doi:10.1007/JHEP11(2012)020.

[34] S. Cui, Y. J. Li, G. Z. Xu and K. Y. Liu, “Order- $v^4$  corrections to heavy quark fragmentation to S-wave heavy quarkonium,” [arXiv:2512.20539 [hep-ph]].

[35] G. T. Bodwin, X. Garcia Tormo, i and J. Lee, “Factorization in exclusive quarkonium production,” Phys. Rev. D **81**, 114014 (2010) doi:10.1103/PhysRevD.81.114014 [arXiv:1003.0061 [hep-ph]].

[36] M. Tanabashi *et al.* [Particle Data Group], “Review of Particle Physics,” Phys. Rev. D **98** (2018) no.3, 030001 doi:10.1103/PhysRevD.98.030001

[37] M. Gremm and A. Kapustin, “Annihilation of S wave quarkonia and the measurement of alpha-s,” Phys. Lett. B **407**, 323-330 (1997) doi:10.1016/S0370-2693(97)00744-2 [arXiv:hep-ph/9701353 [hep-ph]].

[38] K. Y. Liu, Z. G. He and K. T. Chao, “Inclusive charmonium production via double  $c\bar{c}$  in  $e^+e^-$  annihilation,” Phys. Rev. D **69** (2004), 094027 doi:10.1103/PhysRevD.69.094027 [arXiv:hep-ph/0301218 [hep-ph]].

[39] Sheng-Juan Jiang, “Revisit the relativistic corrections to inclusive  $J/\psi$  production at B factories”, [In preparation].